INFLUENCE OF METEOROLOGICAL TIME FRAME AND VARIATION ON HORIZONTAL DISPERSION COEFFICIENTS IN GAUSSIAN DISPERSION MODELING

B. K. Fritz, B. W. Shaw, C. B. Parnell, Jr.

ABSTRACT. *The air pollution regulatory process involves the permitting of sources of regulated pollutants. This process requires sources to demonstrate that the National Ambient Air Quality Standards (NAAQS) are not exceeded as a result of released pollutants. A determination of a facility's compliance with the NAAQS is more frequently being based on dispersion modeling estimates rather than ambient air sampling results. Current Gaussian-based dispersion models do not adequately account for pollutant dispersion due to sub-hourly variations in wind speed and direction. This can result in overestimates of downwind concentration and consequentially require costly additional control measures or denial of a construction or operating permit. This research focuses on developing a methodology to analyze the theoretical degree of dispersion within sub-hourly and hourly intervals. The methodology employed to develop the presently used Pasquill-Gifford (PG) dispersion coefficients is explored and used in developing a new methodology for estimating theoretical dispersion coefficients based on recorded meteorological data. This comparison allowed for an appropriate application time period of the PG dispersion coefficients to be determined, which in general varied from 3 to 20 min. The most critical result of this research is that universal application of the PG dispersion coefficients to a 1 h time period is incorrect. This misapplication will result in concentration estimates based on insufficient plume spread, which will overestimate downwind concentrations and result in inappropriate regulation of emitting sources.*

Keywords. *Atmospheric stability, Dispersion modeling, Gaussian modeling, Pasquill stability parameters, Plume spread, Stability parameter.*

The Federal Clean Air Act (FCAA) of 1960 and subsequent amendments established national goals for air quality and incorporated the use of standards for the control of pollutants in the environment. The 1970 FCAA Amendments (FCAAA) provided the authority to create the Environmental Protection Agency (EPA) and required the EPA to establish National Ambient Air Quality Standards (NAAQS) (U.S. EPA, 1996). The NAAQS are composed of primary standards (based on protecting against adverse health effects of listed criteria pollutants among sensitive population groups) and secondary standards (based on protecting public welfare, e.g., impacts on vegetation, crops, ecosystems, visibility, climate, man-made materials, etc.) The FCAA is the predominate piece of legislation that provides State Air Pollution Regulatory Agencies (SAPRA) the authority to regulate sources of air pollution. These regulatory programs have traditionally fallen into three categories: prohibition of new and existing sources emitting pollution in excess of the ambient air quality standards, controls and permitting requirements for new sources, and specific pollution problems such as hazardous air pollutants and visibility impairment (Brownell, 1999).

The current regulatory process requires sources to demonstrate, by either sufficient sampling or dispersion modeling, that the source's off-property concentrations do not exceed the NAAQS. In a recent effort in permitting a cotton gin, the regulatory entity opted to base the permit requirements on modeling results as compared to on-site sampling results. Given that a source's right to operate could hinge primarily on modeled property-line concentration estimates, it is essential that the most appropriate model be applied.

Industrial Source Complex (ISC) is the model currently used by most SAPRAs for low-level point sources such as cotton gins, feed mills, and grain elevators, as well as larger industrial sources such as power plants. ISC, like many EPA-approved models, is a Gaussian-based model. The accuracy of Gaussian-based dispersion models has long been debated (Beychok, 1996). One major issue associated with the models' accuracy relates to determining the most appropriate time averaging period to use in defining plume spread (Williams, 1996; Beychok, 1994). The primary parameters involved in defining the degree of plume spread as a function of averaging time are the dispersion coefficients (σ_y and σ_z), which are directly related to the plume height and width, respectively, at any point downwind of the source.

This article focuses on the development of the commonly accepted and used Pasquill-Gifford (PG) dispersion coefficients, with emphasis on the horizontal dispersion coeffi-

Article was submitted for review in November 2003; approved for publication by the Structures & Environment Division of ASAE in March 2005.

The authors are **Bradley K. Fritz, ASAE Member Engineer,** Agricultural Engineer, USDA-ARS, College Station, Texas; **Bryan W. Shaw, ASAE Member Engineer,** Associate Professor, and **Calvin B. Parnell, Jr., ASAE Fellow,** Regents Professor, Department of Biological and Agricultural Engineering, Texas A&M University, College Station, Texas. **Corresponding author:** Bradley K. Fritz, USDA-ARS, 2771 F&B Road, College Station, TX 77845; phone: 979-260-9584; fax: 979-260-9386; e-mail: bfritz@apmru.usda.gov.

cient. Mathematically, these parameters are the standard deviations of a normally distributed plume in the horizontal and vertical planes, and are correlated to atmospheric stability. For example, unstable atmospheric conditions correspond to greater wind speed and direction variations than stable atmospheric conditions. Therefore, greater plume spread would be expected under unstable conditions as compared to stable conditions.

The Gaussian Model

All Gaussian-based dispersion models are based on the assumption that the concentration of a pollutant in both the vertical and horizontal plane, at a given downwind distance from a source, can be represented by a normal, or Gaussian, distribution (fig. 1). The degree of spread associated with normal distributions is a function of both the downwind distance and the variation in wind direction and wind speed, and is represented by the dispersion coefficients σ_y and σ_z. Note that the dispersion coefficients (σ_y and σ_z) are the standard deviations associated with the normal distribution in the vertical and horizontal planes, respectively, represented in the Gaussian equation. The general form of the Gaussian dispersion equation is shown in equation 1 (Cooper and Alley, 1994):

$$C = \frac{Q}{2\pi u \sigma_y \sigma_z} \exp\left(-\frac{1}{2}\frac{y^2}{\sigma_y^2}\right)\left\{\exp\left(-\frac{1}{2}\frac{(z-H)^2}{\sigma_z^2}\right) + \exp\left(-\frac{1}{2}\frac{(z+H)^2}{\sigma_z^2}\right)\right\} \quad (1)$$

where

C = steady-state concentration at a point (x,y,z) ($\mu g/m^3$)
Q = emission rate ($\mu g/s$)
σ_y = horizontal dispersion coefficient (m)
σ_z = vertical dispersion coefficient (m)
u = wind speed at stack height (m/s)
y = horizontal distance from plume centerline (m)
z = height of receptor with respect to ground (m)
H = effective stack height (m, $H = h + \Delta h$, where h = physical stack height, and Δh = plume rise).

Notice that the Gaussian equation is simply the ratio of emission rate over wind speed multiplied by two normal density functions: one for the horizontal direction, and the other for the vertical direction. Assuming that all source parameters are available and the desired receptor locations are known, the only unknowns in the Gaussian equation are wind speed and the dispersion coefficients. Wind speed is obtained directly from meteorological data, and the dispersion coefficients are determined based on the degree of recorded atmospheric stability.

Atmospheric Stability Classification and Dispersion Coefficients Estimates

The Pasquill-Gifford (PG) dispersion coefficients associate observed plume spread data with the Pasquill atmospheric stability classes (Seinfeld and Pandis, 1998). The most frequently used classification system of atmospheric stability was developed by Pasquill (U.S. EPA, 1996). These stability classes were developed to allow the Gaussian dispersion equation to be evaluated with readily available, simple meteorological data (Pasquill and Smith, 1983). The stability classes represent different meteorological turbulence conditions, which correspond to wind speed ranges and either solar radiation (daytime) or cloud cover (nighttime) (Barratt, 2001; Pasquill and Smith, 1983), as shown in table 1.

There is some difference of opinion surrounding the time period of application associated with the PG dispersion coefficients. The most appropriate application time period would be that for which the individual plume spread concentration data were recorded. Present models, such as ISC version 3 (ISC3), apply the dispersion coefficients to

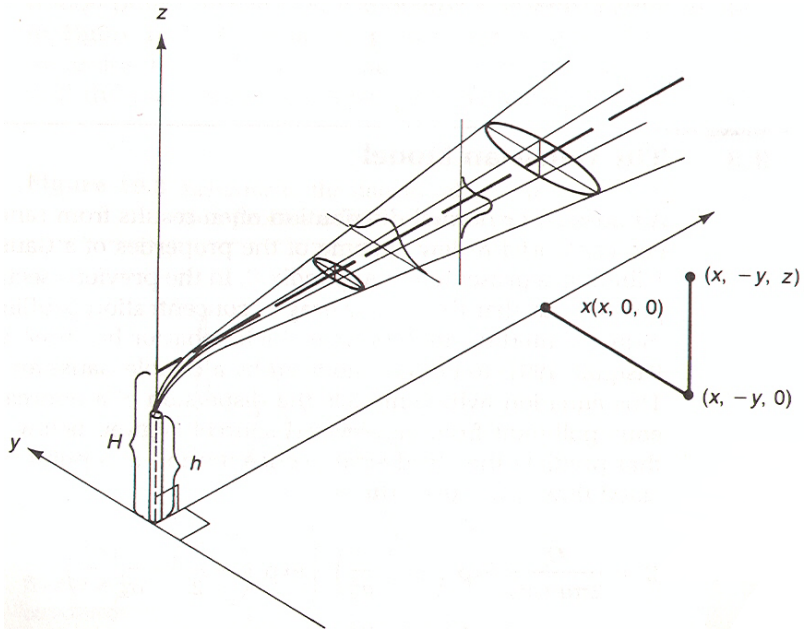

Figure 1. Graphical representation of normal distributions in the vertical and horizontal planes in the Gaussian dispersion model (Cooper and Alley, 1994).

Table 1. Stability classifications (Cooper and Alley, 1994).

Surface Wind Speed (m/s)	Solar Radiation[a] (Day)			Cloud Cover (Night)[b]	
	Strong	Moderate	Slight	Cloudy (≥4/8)	Clear (≤3/8)
<2	A	A-B[c]	B		
2-3	A-B	B	C	E	F
3-5	B	B-C	C	D[d]	E
5-6	C	C-D	D	D	D
>6	C	D	D	D	D

[a] Strong insolation corresponds to sunny midday in midsummer in England; slight insolation corresponds to similar conditions in winter.
[b] Night refers to the period from 1 h before sunset to 1 h after sunrise.
[c] For A-B, etc., take the average of the values for A and B.
[d] The neutral class (D) should also be used, regardless of wind speed, for overcast conditions during day or night and for sky conditions during the hour preceding or following night, as defined above.

calculate 1 h concentration estimates, while the classical Gaussian dispersion equation (applying the PG stability parameters) is cited to return 10 min concentrations (Cooper and Alley, 1994). Williams (1996) demonstrated that 1 h concentration values obtained from the ISC Screen3 (a simplified screening algorithm) model equaled the 10 min Gaussian dispersion model (eq. 1) concentrations.

There have been other interpretations of the application time period for the PG dispersion coefficients. Zannetti (1990), referencing Gifford (1961), stated that σ_y and σ_z were derived based on concentration readings taken every 3 min. Pasquill (1961) also denotes that the plume concentration measurements used in developing the dispersion coefficients were based on 3 min source releases. Venkatram (1995), alluding to the Project Prairie Grass experiment that was the basis for Pasquill's dispersion coefficient estimates, states that the experiment consisted of tests lasting about 10 min in length. Cooper and Alley (1994) explicitly state that the "concentration predicted by [the Gaussian model], using the σ_y and σ_z values from [the Pasquill-Gifford-Turner curves] is a 10-minute-averaged concentration." Given the variation of time periods cited in the literature, there is no universally agreed upon time of application. Beychok (1996) provided a good summation of this issue, which is restated in the following paragraph:

"A major problem with the Gaussian dispersion equation is defining what the calculated concentration *C* represents when using Pasquill's dispersion coefficients. D. B. Turner states that *C* represents a 3- to 15-minute average; and American Petroleum Institute dispersion modeling publication believes *C* represents a 10- to 30-minute average; S. R. Hanna and P. J. Drivas believe *C* is a 10-minute average; and others attribute averaging times from 5 minutes to 30 minutes. Most agree on a range of 10 minutes to 15 minutes. However, many Environmental Protection Agency computer models used to determine regulatory compliance assume that the Gaussian dispersion equation yields 60-minute averaged concentrations."

The original development of the dispersion coefficients relied on visual observations of plume spread resulting from test releases. The visible edge of the plume was defined as the point at which the concentration was 10% of the centerline (maximum) concentration (Gifford, 1961). Assuming the crosswind plume concentration is normally distributed with the ordinate at the plume centerline, an expression relating concentration at some distance from the ordinate as a percentage of the ordinate concentration can be developed. Using the normal density function and trigonometric relationships, the value of the horizontal stability parameter (σ_y), which is the standard deviation associated with the horizontal distribution in the Gaussian equation, can be expressed in terms of the degree of plume spread (θ) and the downwind distance (x) from the source (Gifford, 1961). Gifford (1961) presented this relationship as a means of calculating σ_y based on observed plume spread data. This relationship is shown in equation 2:

$$\sigma_y = \frac{x \cdot \tan\left(\frac{\theta}{2}\right)}{2.15} \quad (2)$$

Plume spread (θ) is dependent on the stability class. Pasquill's (1961) estimates of θ for each stability class are given in table 2. These values are based on data collected during Project Prairie Grass. This project consisted of 70 trials conducted in the summer of 1956 in flat, open prairie country in north-central Nebraska. Each of the 70 trials consisted of releasing sulfur dioxide continuously for several minutes. As the gas plume moved downwind, sensors located along arcs from 50 to 800 m downwind measured the sulfur dioxide content. These observations, along with observations from other similar experiments, were used to develop equations describing plume spread under different atmospheric stability classes.

As previously noted, the dispersion coefficient values were determined based on observed data, and were developed only as estimates to be used when vertical and horizontal wind direction fluctuation data were unavailable. Pasquill (1961) recommended using the fluctuation data over the estimated data. The observed plume spread and plume height values reported by Pasquill (1961) were based on observations resulting from "short releases (a few minutes)" (Pasquill, 1961). Turner (1994) interpreted "a few minutes" as approximately 10 min. Turner (1994) states Pasquill later clarified the averaging time as being 3 min. Trinity Consultants (2000), a leading developer of the Industrial Source Complex (ISC) model, stated that "if these parameters are used for hourly periods, they are representing those rather extreme hourly periods in which the wind is steady and the mean wind directions of the 20 three-minute periods in the hour are all the same."

In order to address this issue, Zwicke (1998) incorporated 2 min meteorological data (averaged wind speed and direction) into the modeling algorithm. Zwicke (1998) conducted a series of controlled pollutant release and measurement tests. Each release was modeled using ISC Short Term (ISCST) and a new model (Gaussian dispersion equation, with *C* being equal to a 2 min concentration). The modeled concentrations were compared to the measured values. Zwicke (1998) reported that ISCST overpredicted the measured concentrations by 2.5 to 10 times, while the new

Table 2. Pasquill's (1961) estimates of lateral plume spread (θ, in degrees) by stability classification and downwind distance.

Downwind Distance (km)	Stability Class					
	A	B	C	D	E	F
0.1	60	45	30	20	15	10
100	20	20	10	10	5	5

model predictions were approximately 2.5 times the measured concentrations. The major challenge associated with this model was the requirement for refined meteorological data (2 min averages versus 1 h averages), as most State Air Pollution Regulatory Agencies (SAPRAs) collect meteorological data in 1 h intervals. Using 1 h meteorological data is in accordance with the EPA guidelines entitled Meteorological Monitoring Guidance for Regulatory Modeling Applications (U.S. EPA, 2000).

OBJECTIVES

The major emphasis of this article is to examine the form and function of the horizontal dispersion coefficient (σ_y). Beychok (1994) reasons that the vertical dispersion coefficient (σ_z) would remain constant regardless of averaging time, as the standard deviation of the vertical wind direction will show very little increase over long sampling times. This article focuses on a methodology for estimating an appropriate time reference for which the theoretical degree of dispersion matches that estimated using the PG horizontal dispersion coefficient.

METHODS

A theoretical "tracer" tracking model was developed to determine plume spread based on recorded meteorological data. Based on the determined theoretical plume spread over a number of averaging times, corresponding dispersion coefficients were calculated. These theoretical dispersion coefficients were compared to the PG dispersion coefficients for each averaging time as a means of evaluating the degree of meteorological variation accounted for by each class of PG dispersion coefficients. Graphical analysis of the resulting data allowed for inferences to be made on time averaging periods most suited to the PG dispersion coefficients for the meteorological data used in the analysis. The developed methodology will be used in future research to calculate dispersion coefficients for specific averaging times and meteorological data characteristics. These steps are explained in greater detail in the following sections.

DEGREE OF PLUME SPREAD AS A FUNCTION OF TIME

The analysis algorithm developed as a part of this research to estimate plume spread based on recorded meteorological data assumes that the spread of a pollutant in the air is predominately convection driven. In other words, the pollutant diffusion as it travels downwind is negligible when compared to wind transport. It was also assumed that the pollutant's travel speed and direction are dictated by wind speed and direction, and changes in travel speed and direction are instantaneous with changes in wind speed and direction.

For this study, meteorological data were collected in 15 s intervals using a Campbell Scientific CR10X datalogger with sensors for temperature, relative humidity, barometric pressure, solar radiation, wind speed, and wind direction. The meteorological station was set up in the middle of a large, flat, open, grass field in College Station, Texas. Data were downloaded daily from 20 February through 25 March 2002. Although monitoring was constant throughout this time period, due to technical problems with the power supply and the wind speed and direction sensors, only 22 full days of meteorological data were collected. As part of the data reduction process, wind speed and direction data for any calm periods (<0.5 m/s, the threshold of the wind speed sensor) were replaced with values based on averages of wind speed and direction from the nearest (timewise) non-calm period that preceded the calm period. For multiple calm periods, wind speed and direction data were based on averages of the nearest non-calm period preceding the group of calm periods. The U.S. EPA (2000) recommends replacing calm periods with the threshold wind speed (1 m/s in referenced document) for use in Gaussian-based modeling. The averaging method presented here was used to provide better continuity of the meteorological data.

Using the collected meteorological data, "tracer" paths were traced from a common point of origination (i.e., the source), and were tracked as they traveled downwind. Tracers are used as entities with no inherent properties whose travel paths are dictated by instantaneous changes in wind speed and direction of the associated time period. Tracers neither grew nor diffused into the surrounding air volume, nor had any interaction affects with the surrounding air volume. Additionally, topography was not considered in tracer paths, i.e., topography was assumed to be flat and level.

Tracers were released at the beginning of each meteorological data interval. For example, at time $t = 0$, tracer 1 was released, and at time $t = 15$ s, tracer 2 was released. All tracers originated at the origin (0,0). The travel path of each tracer was tracked mathematically based on the average wind speed and direction recorded for each 15 s interval. For each time interval, the distance traveled was determined using the wind direction, wind speed, and time interval ($t = 15$ s).

These tracer paths were used to determine the plume spread at various downwind distances. A tracer path plot based on a 10 min period of collected meteorological data is shown in figure 2. Each individual tracer path in figure 2 resulted from tracing a unique parcel release and its subsequent downwind travel as a result of wind speeds and directions from the subsequent time intervals. The distances in the horizontal plane and the average wind direction for the period were used to establish a line perpendicular to the average wind direction at a distance from the source that corresponds to the downwind distance. The point where the average wind direction vector and the perpendicular downwind line intersect was denoted as the plume center. Figure 3 is a simplified illustration showing how, for each parcel path crossing, the length from the plume center (I2) to the point in the plume where the tracer crosses (I1) was determined. This length is denoted as *W* and was determined for each tracer path. For a given time period, *W* can be plotted and fitted to a normal distribution, as shown in figures 4 and 5. From this fit, the plume spread parameter (σ_y), referred to as $\sigma_{y\ BKF}$, can be determined.

When determining the total plume spread based on the *W* values, the associated time period was based on the number of tracers crossing the downwind distance line. For instance, a 2 min concentration based on 15 s interval meteorological data would require eight tracers crossing the line representing the downwind distance (8×15 s = 120 s = 2 min). For initial iterations, total plume width values were calculated for each time interval using only meteorological data for the time period of interest. For example, a 3 min block of meteorological data would be used for a 3 min plume width. This approach resulted in some plume widths that were based on fewer than the required number of *W* values (i.e., a 3 min

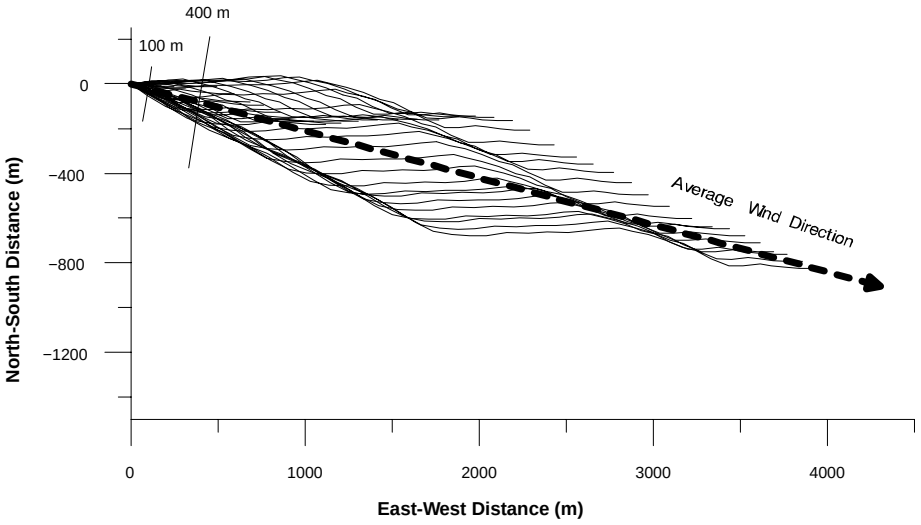

Figure 2. Theoretical 10 min tracer path in the horizontal plane using measured 15 s interval meteorological data. Tracer path lines are extending in the averaged direction of the wind.

plume width should be based on 12 tracer crossings, whereas some were based on less than 12). The reason for this deficit in *W* values was the lag time associated with the transport of the tracer from the source to the downwind line. For example, for a 2 m/s wind speed, a tracer will only travel 30 m in one 15 s time interval (2 m/s × 15 s = 30 m). If the wind speed remained constant for the remaining time intervals, four 15 s intervals would be required for the tracer to cross the 100 m downwind line, assuming straight-line travel. When the downwind distance is 500 to 1000 m, the lag time becomes quite large. At large downwind distances, there are no tracer crossings within the set time period. Lag time was incorporated to account for this problem.

For a specific time interval, a clock was started after the first tracer crossed the downwind line. When the clock indicated the specified time interval had elapsed, plume tracing was stopped. The plume width was calculated based on the tracer crossings (*W*) recorded during the analysis.

As an example, for a given hour of meteorological data, the 10 min plume widths are to be calculated. Examining the first 10 min of data at 500 m downwind, for a wind speed of 3 m/s, the first tracer would not cross the downwind line until a minimum 2 min and 47 s had elapsed. Assuming a tracer crossed every 15 s for the remaining data intervals, the 10 min plume width would actually be based on 12 to 13 min of meteorological data. Similarly, a 60 min plume width might be based on more than 60 min worth of meteorological data. The average and standard deviations of wind direction and speed were based on the total time period over which plume tracing occurred. As such, the 10 min plume width mentioned above would be associated with meteorological data statistics for 12 to 13 min.

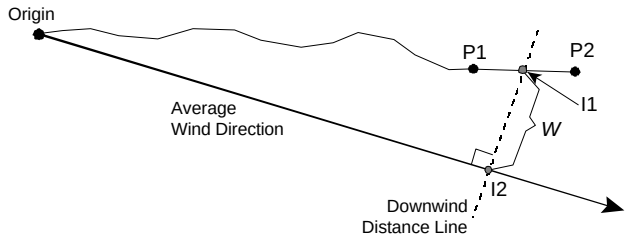

Figure 3. Graphical representation of the methodology used to calculate *W* using theoretical tracer path data: P1 and P2 are initial and final (*x*,*y*) coordinates of the parcel's last incremental movements, I1 is the (*x*,*y*) coordinate where the P1-P2 vector intersects the downwind distance line, I2 is the (*x*,*y*) coordinate where the average wind direction line (i.e., plume centerline) intersects the downwind distance line, and *W* is the distance between I1 and I2.

The *W* values for each time period of interest were then fit to a normal distribution (to meet the assumption of a normally distributed plume associated with Gaussian modeling), and the standard deviation were determined. As an example, for a given hour, the first step was to calculate *W* values and meteorological statistics (incorporating data from the lag time period) for each consecutive 2 min data period, and then to fit the *W* data for each period to a normal distribution and determine the associated standard deviation (denoted σ_y). This process was then repeated for 3 min data intervals, for 5 min data intervals, etc., up to a single 60 min data interval corresponding to each hour. Note that for each individual time period, the data interval stability classification (which will be discussed in the next section) was determined.

Figures 4 and 5 are based on the example plume trace in figure 2. The standard deviation associated with the normal distribution fitted to the *W* values is 18.6 m at 100 m downwind for a 10 min period (fig. 4). Similarly, for 400 m, the standard deviation (σ_y) is 64.3 m (fig. 5).

This methodology was used to develop a FORTRAN program to perform similar data reduction over the entire set of meteorological data. Each hour of collected meteorological data was analyzed for 2, 3, 5, 10, 15, 20, 30, and 60 min intervals, and at 100, 200, 300, 400, 500, 600, 700, 800, 900, and 1000 m downwind. For each interval and downwind distance combination ($\sigma_{y\ BKF}$), average values of wind speed, wind direction, and solar radiation and the standard deviations of wind speed and wind direction were determined. The meteorological data statistics incorporate the lag time period's meteorological data, as discussed earlier.

Estimation of Stability Classification

The next step was to compare the $\sigma_{y\ BKF}$ values to the corresponding $\sigma_{y\ PG}$ (the horizontal PG dispersion coefficient) values for each stability class, time interval, and

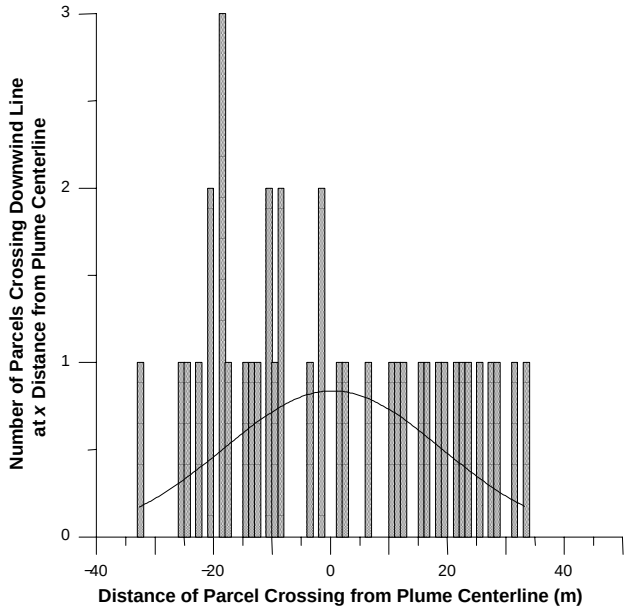

Figure 4. Histogram and normal distribution fit of plume width values (*W*) as determined from theoretical parcel trace data at 100 m downwind ($\sigma_{y\ BKF}$ = 18.6 m).

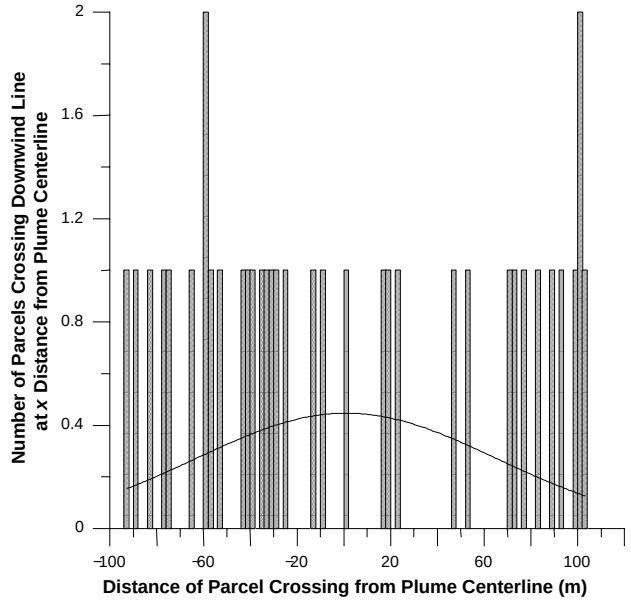

Figure 5. Histogram and normal distribution fit of plume width values (*W*) as determined from theoretical parcel trace data at 400 m downwind ($\sigma_{y\ BKF}$ = 64.3 m).

downwind distance combination. The stability class for each interval of data was determined in order to calculate $\sigma_{y\ PG}$. There are several methods available for estimating the PG stability classification using measured meteorological data. The first method employed was the solar radiation/ΔT (SRDT) method (U.S. EPA, 2000). This method differentiates daytime stability classes using the measured solar radiation (W/m^2) and wind speed ranges (m/s), as indicated by the EPA's Meteorological Monitoring Guidelines (U.S. EPA, 2000). Likewise, the nighttime stability classifications are differentiated using the ΔT (vertical temperature gradient) and wind speed ranges (U.S. EPA, 2000). The second method

Table 3. Summary statistics of meteorological data used in time frame analysis study.

Stability Class	Total Hours during 22 Day Period	Average Wind Speed (m/s)	Wind Speed Standard Deviation (m/s)	Wind Direction Standard Deviation (°)
B	41	2.7	0.94	28.4
C	121	3.8	0.85	14.3
D	328	3.8	0.77	10.2
E	46	2.6	0.43	7.1
F	6	1.5	0.37	13.6

Table 4. Total number of data points for each time interval of interest within each stability class.

Stability Class	Time Interval (min)							
	2	3	5	10	15	20	30	60
B	1230	820	492	246	164	123	82	41
C	3630	2420	1452	726	484	363	242	121
D	9840	6560	1936	1968	1312	984	656	328
E	1380	920	552	276	184	138	92	46
F	180	120	72	36	24	18	12	6

used to estimate the PG stability classes is referred to as the SigmaA (standard deviation of the horizontal wind direction) method (U.S. EPA, 2000).

Both of these methods were used and compared against each other using the 1 h averaged data for each hour of collected data. It was found that for estimates of daytime stability using the measured meteorological data, 75.7% of the estimates from the two methods agreed and 93.4% of the estimates were within one stability class of each other. For the nighttime stability class determination, only the SigmaA method was employed, as the temperature gradient required temperature measurements at heights of $20z_o$ to $100z_o$ (where z_o is the surface roughness height, about 0.03 m for the present location), which were unavailable. For the purpose of assigning a stability class for determining the PG stability parameter, the solar radiation method was used for daytime meteorological data intervals (solar radiation >0 W/m^2) and the SigmaA method was used for nighttime meteorological data intervals (solar radiation <0 W/m^2).

Results and Discussion

For each hour of measured meteorological data, $\sigma_{y\ BKF}$, $\sigma_{y\ PG}$, and the ratio of $\sigma_{y\ PG}/\sigma_{y\ BKF}$ were determined for each time interval and downwind distance combination. For example, for a given hour of meteorological data, using 2 min time intervals, there would be 30 data sets with $\sigma_{y\ BKF}$, $\sigma_{y\ PG}$, and the ratio of $\sigma_{y\ PG}/\sigma_{y\ BKF}$, with each set of data being representative of a different 2 min interval. Similarly, for the 3, 5, 10, 15, 20, 30, and 60 min time intervals, the number of data sets would be 20, 15, 6, 3, 2, and 1, respectively. When $\sigma_{y\ BKF}$ equals $\sigma_{y\ PG}$, the ratio equals 1 and the associated time interval and degree of meteorological variation is equivalent to that accounted for by the horizontal PG dispersion coefficient. If the ratio is greater than 1, then the horizontal PG dispersion coefficient overestimates the plume spread. For a ratio less than 1, the plume spread is underestimated by the horizontal PG dispersion coefficient. For example, for given a 5 min interval, if $\sigma_{y\ BKF}$ and $\sigma_{y\ PG}$ are equal, then the horizontal PG dispersion coefficient could be appropriately applied. For each stability class, time interval, and downwind

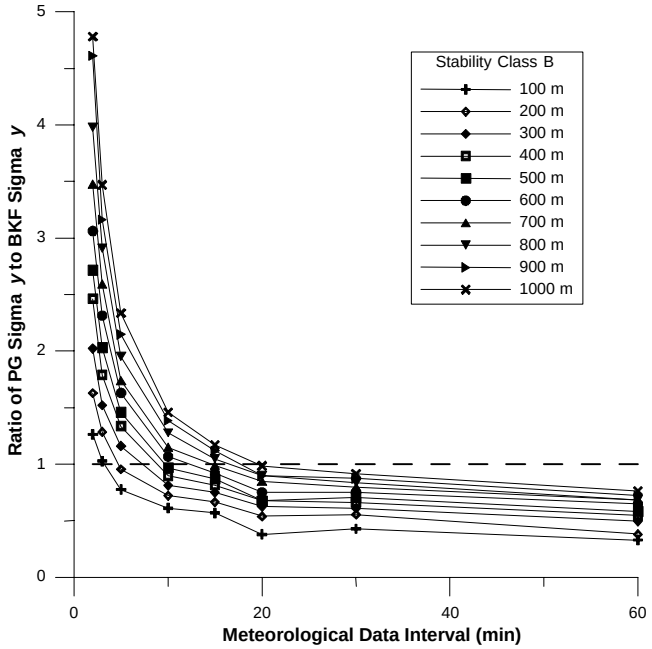

Figure 6. Ratio of $\sigma_{y\ PG}$ to $\sigma_{y\ BKF}$ for stability class B as a function of meteorological data, time interval, and downwind distance from the source.

distance combination, the average and standard deviation of the ratio data were determined. It should be noted that no data were available for stability class A, as there were no complete hours that were classified as such. Table 3 is a summary of the meteorological data by stability classification. Figures 6 through 10 are plots of the ratio of $\sigma_{y\ PG}$ to $\sigma_{y\ BKF}$ for each stability class and each downwind distance within each stability class. The number of data points averaged for each point plotted in figures 6 through 15 can easily be determined by taking the total number of hours within the given stability class and multiplying by the number of data sets for each time interval. These values are given in table 4.

In general, the time interval of agreement (where the ratio is equal to 1; represented in the graphs by a dotted line) is between 2 and 40 min for all stability classes. For all stability classes, as the distance from the source increases, the time interval of agreement also increases. The reason for this is that the further a receptor is from a source, the less will be the impact due to variations in meteorological conditions. From these graphs, it can be concluded that applying the horizontal

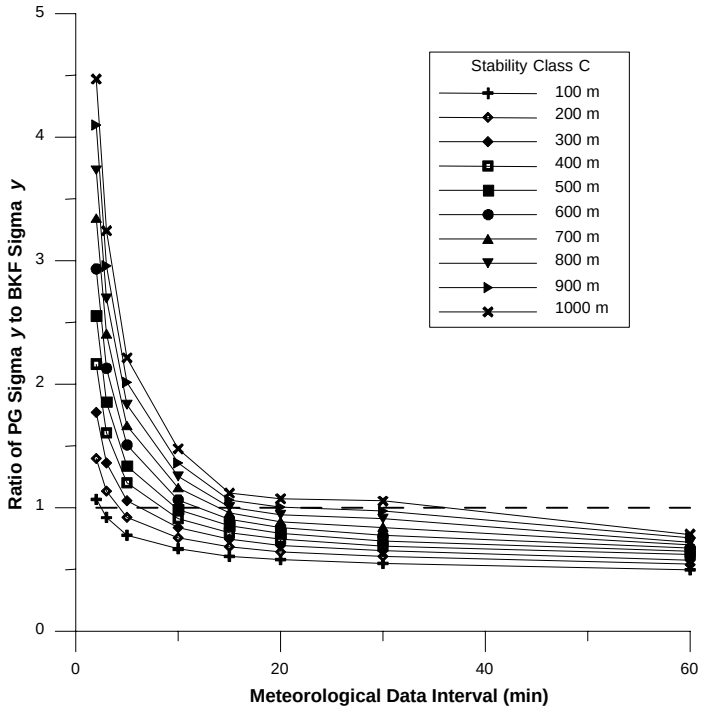

Figure 7. Ratio of $\sigma_{y\ PG}$ to $\sigma_{y\ BKF}$ for stability class C as a function of meteorological data, time interval, and downwind distance from the source.

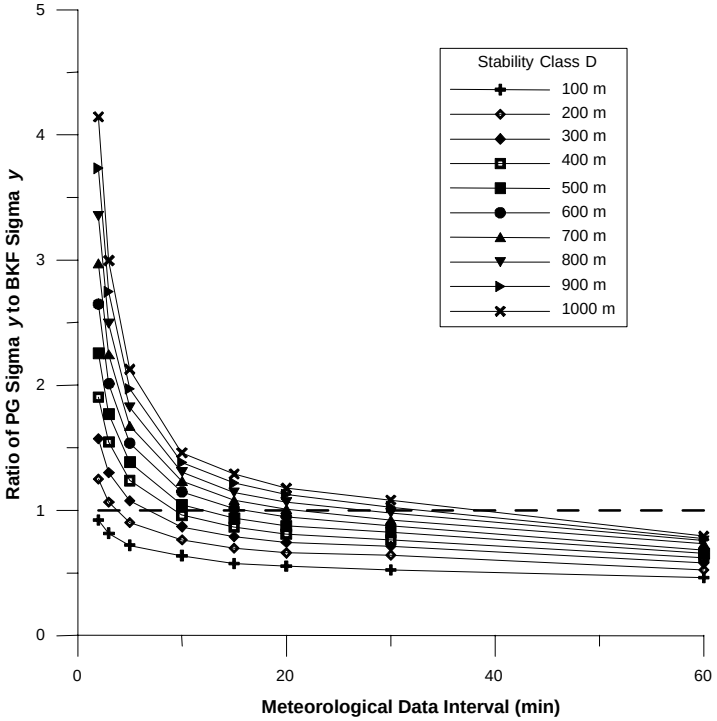

Figure 8. Ratio of $\sigma_{y\ PG}$ to $\sigma_{y\ BKF}$ for stability class D as a function of meteorological data, time interval, and downwind distance from the source.

PG dispersion coefficient to a 1 h time period is not appropriate and will result in concentration predictions that are excessive (i.e., $\sigma_{y\ PG}$ is smaller than $\sigma_{y\ BKF}$; thus, the associated degree of plume spread will be less). Figures 11 through 15 are plots of the $\sigma_{y\ BKF}$ values with 95% confidence intervals along with the $\sigma_{y\ PG}$ values for each stability class, downwind distance, and time interval combination.

When examining figures 11 through 15, notice how the value of $\sigma_{y\ BKF}$ changes with the time interval of applied meteorological data. As the time interval of the meteorological data increases, both the mean and the confidence interval associated with $\sigma_{y\ BKF}$ increase. In addition, as the distance from the source increases, the widths of the $\sigma_{y\ BKF}$ confidence intervals increase. In general, as the meteorological time interval increases, the average value of $\sigma_{y\ BKF}$ also increases. Notice also that for stability class F (fig. 15) the mean and the confidence interval of $\sigma_{y\ BKF}$ increase greatly with time interval and downwind distance, much more so than for the

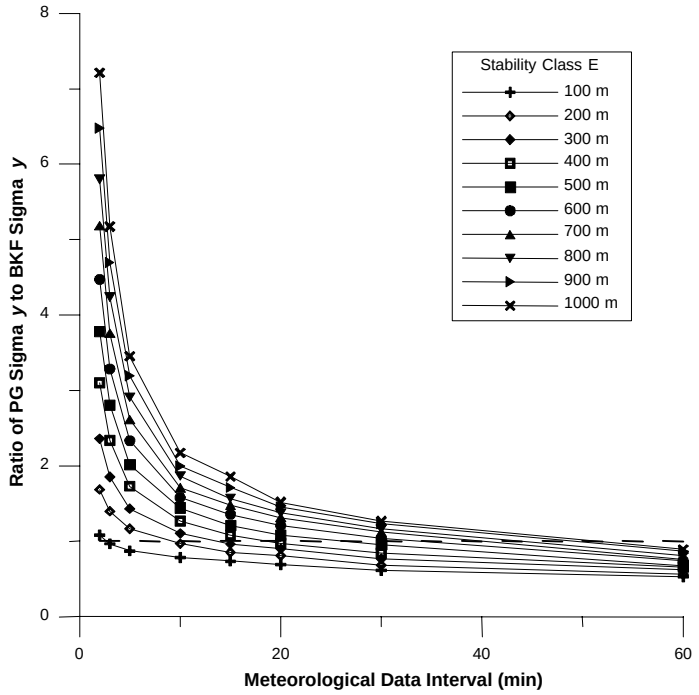

Figure 9. Ratio of $\sigma_{y\ PG}$ to $\sigma_{y\ BKF}$ for stability class E as a function of meteorological data, time interval, and downwind distance from the source.

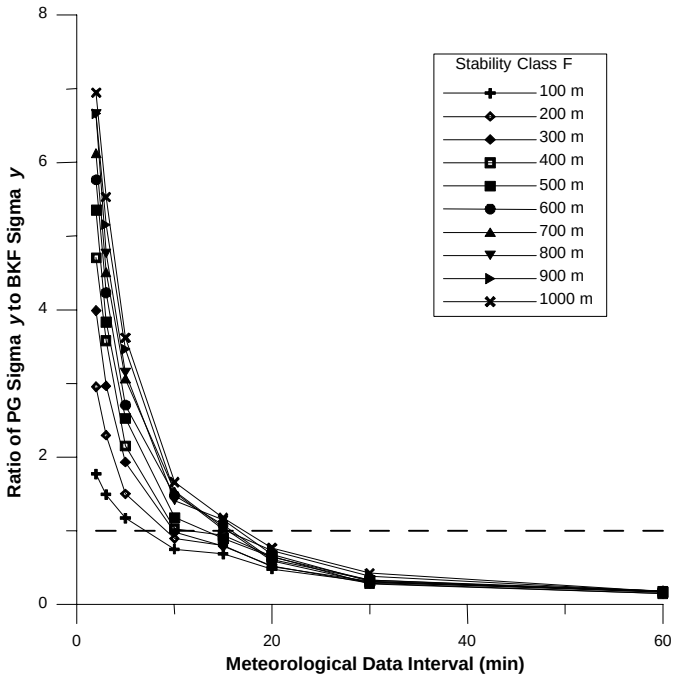

Figure 10. Ratio of $\sigma_{y\ PG}$ to $\sigma_{y\ BKF}$ for stability class F as a function of meteorological data, time interval, and downwind distance from the source.

other stability classes. One reason for this is that stability class F is associated with light and variable winds, which will cause the plume to meander to a greater degree than in other stability classes. As downwind distance increases, this meandering effect has a more significant impact on plume spread. An additional factor is the small number of data points, especially for the longer time intervals, which would result in large confidence intervals, especially given the inherent variability within this stability class.

The most appropriate time frame for each stability class and downwind distance combination can also be observed from figures 11 through 15. For each combination of downwind distance and stability class, the most appropriate time period of application corresponds to the time interval where the mean $\sigma_{y\ BKF}$ is equal to the value of $\sigma_{y\ PG}$. For example, from figure 11 (stability class B) at a distance of 100 m, $\sigma_{y\ BKF}$ and $\sigma_{y\ PG}$ are equal for the 3 min interval data. The actual σ_y values may be greater, lesser, or equal to $\sigma_{y\ PG}$

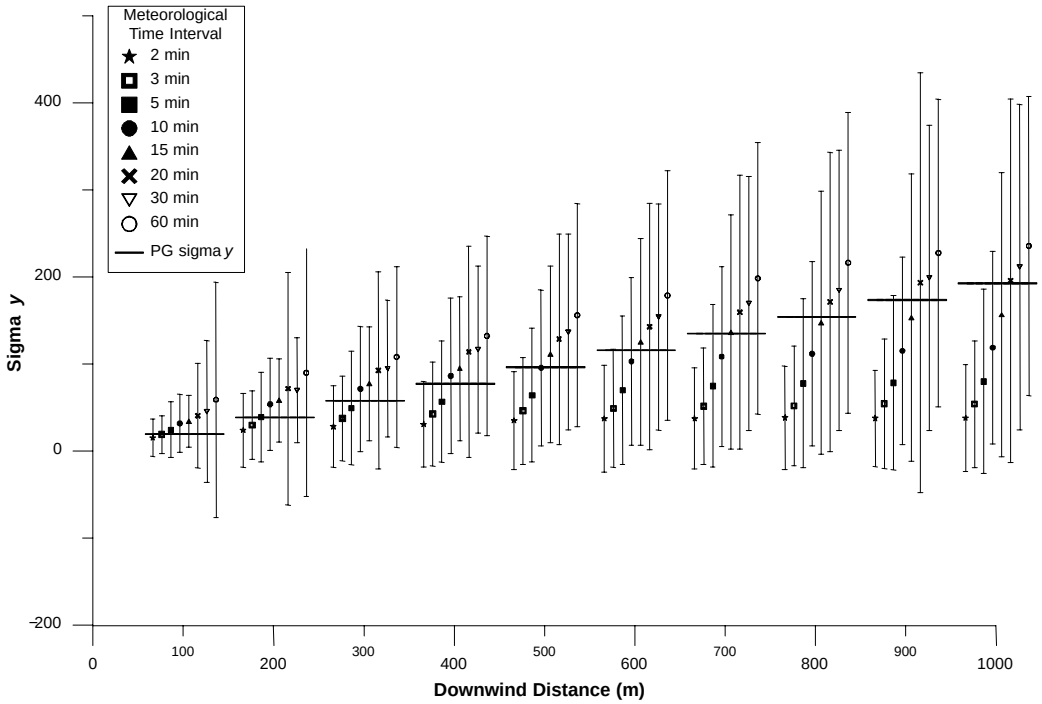

Figure 11. Pasquill-Gifford (PG) σ_y and 95% confidence interval and mean of $\sigma_{y\ BKF}$ by meteorological time interval and downwind distance combinations for stability class B data.

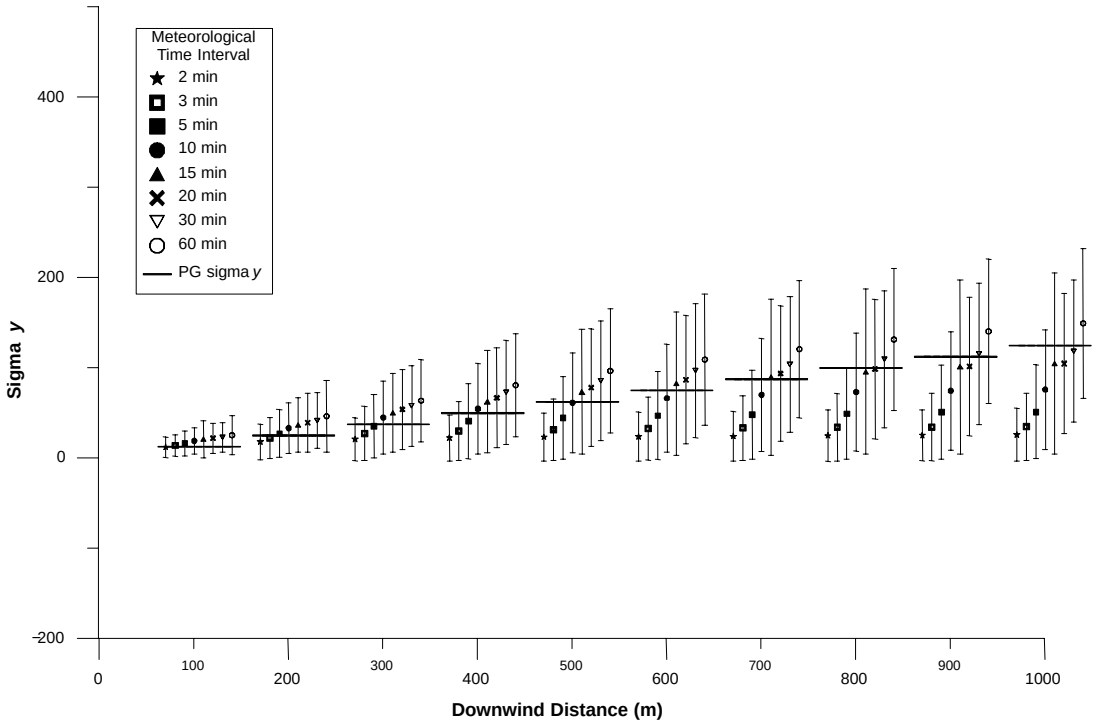

Figure 12. Pasquill-Gifford (PG) σ_y and 95% confidence interval and mean of $\sigma_{y\ BKF}$ by meteorological time interval and downwind distance combinations for stability class C data.

depending on meteorology. For example, for stability class C and 300 m downwind, $\sigma_{y\ PG}$ would be 31.7 m. From this research, the value of $\sigma_{y\ BKF}$ at 300 m downwind based on 1 h of meteorological data classified as stability class C is on average twice the value of $\sigma_{y\ PG}$ and could range from 15 to 110 m (based on fig. 12). Table 5 is a summary of the most appropriate time intervals for the combinations of stability class and downwind distance.

The degree of variation in $\sigma_{y\ BKF}$ differs from one stability class to another. For example, by moving from stability class B to D, the overall variance in σ_{yBKF} decreases, i.e., the width of the $\sigma_{y\ BKF}$ confidence intervals decreases. Further, when

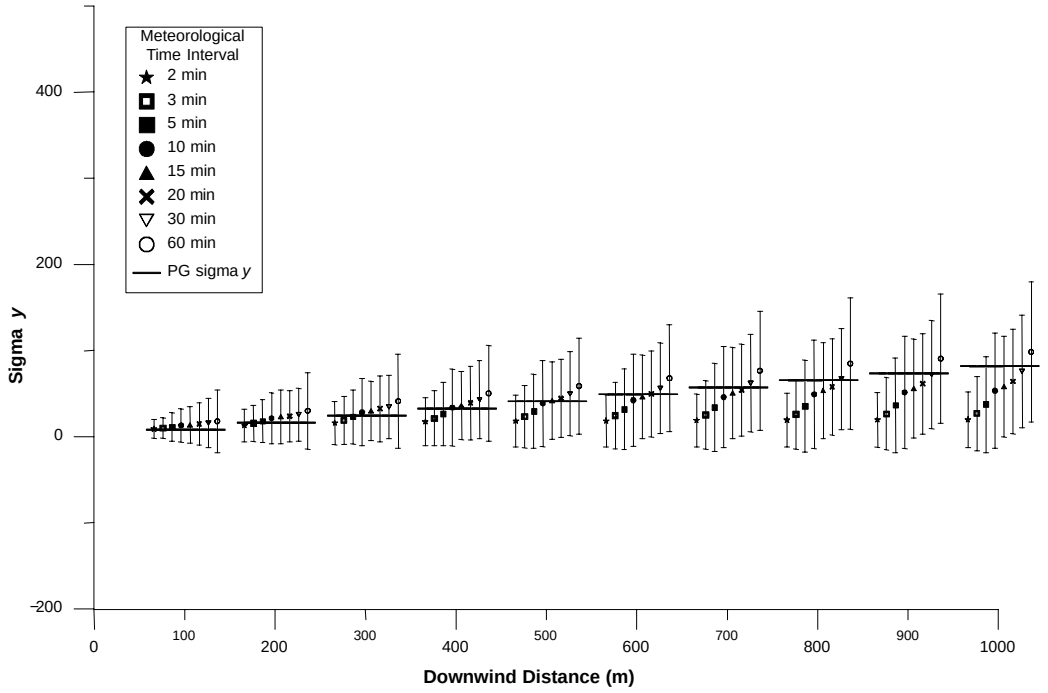

Figure 13. Pasquill-Gifford (PG) σ_y and 95% confidence interval and mean of $\sigma_{y\ BKF}$ by meteorological time interval and downwind distance combinations for stability class D data.

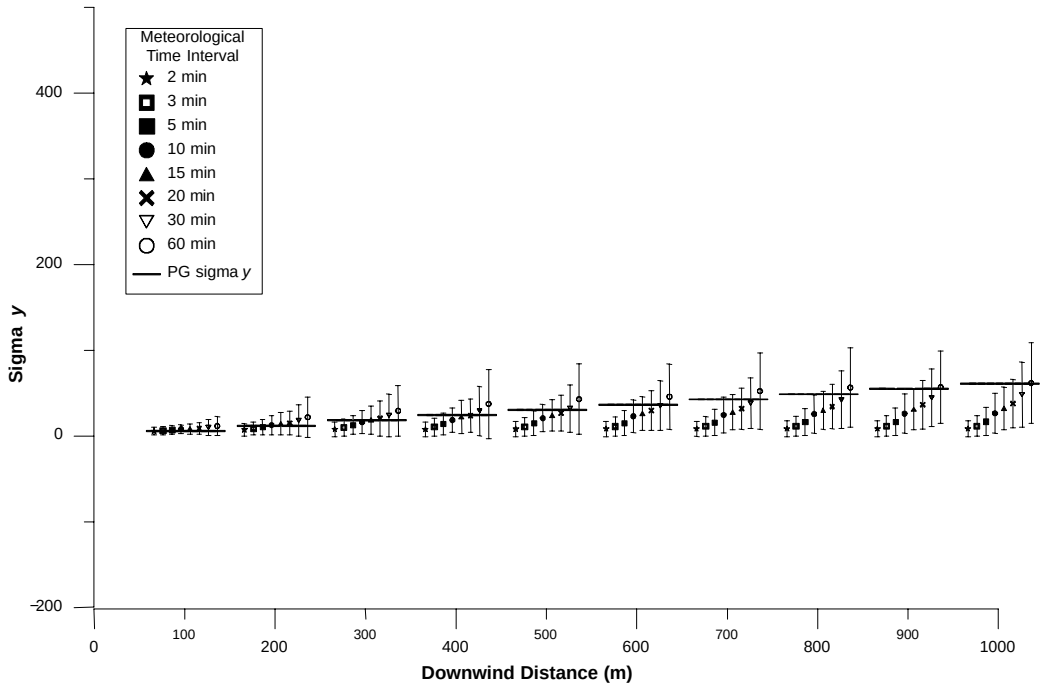

Figure 14. Pasquill-Gifford (PG) σ_y and 95% confidence interval and mean of $\sigma_{y\ BKF}$ by meteorological time interval and downwind distance combinations for stability class E data.

moving from stability class A to D, the stability of the meteorological parameters increases. For example, an hour corresponding to stability class A will have a greater variation in wind direction and a lower wind speed than an hour corresponding to stability class C or D. Therefore, it would be expected that the more stable daytime stability classes (i.e., C and D) would be associated with not only smaller horizontal dispersion coefficients, but also smaller variation in the range of the horizontal dispersion coefficient. This brings up another important point that can be observed from figures 11 through 15. The confidence intervals on $\sigma_{y\ BKF}$ from one stability class to another are not exclusive. In other words, stability classes A, B, or C could all have hours where the degrees of plume spread are equal.

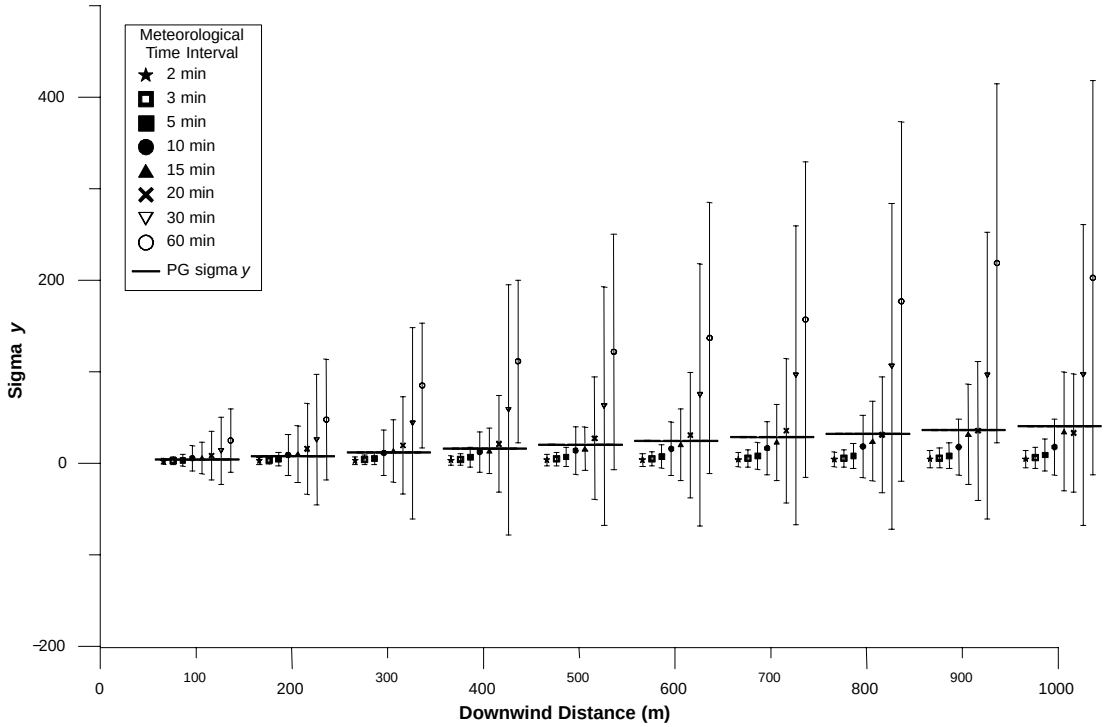

Figure 15. Pasquill-Gifford (PG) σ_y and 95% confidence interval and mean of $\sigma_{y\ BKF}$ by meteorological time interval and downwind distance combinations for stability class F data.

Table 5. Appropriate time intervals (min) for applying the Pasquill-Gifford dispersion coefficient ($\sigma_{y\ PG}$).

Stability Class	Downwind Distance (m)									
	100	200	300	400	500	600	700	800	900	1000
B	3	5	5-10	5-10	10	10-15	15	15-20	15-20	20
C	2-3	3-5	5	5-10	10	10-15	15	20	20-30	30+
D	2	3	5	10	15	20	20-30	30	30	30+
E	2-3	10	15	20	30	30	30-60	30-60	60	60
F	2-15	5-15	10-15	15-20	15-20	15-20	15-20	20	20	20+

CONCLUSION

The goal of this research was the development of a model that accounts for variations in sub-hourly meteorological conditions, yet can be used with hourly meteorological data. The first step in this process was to gain a greater understanding of how, and to what degree, the current models account for these variations. A methodology was developed to determine plume spread for multiple time intervals and downwind distance combinations using small-time-interval (less than hourly) meteorological data. The plume spread values were used to calculate an "observed" horizontal dispersion coefficient ($\sigma_{y\ BKF}$). This observed value was then compared with the Pasquill-Gifford predicted dispersion coefficient ($\sigma_{y\ PG}$). This comparison allowed for an appropriate application time period to be determined, which in general, was less than 20 min.

The most critical finding of this research was that applying the horizontal PG dispersion coefficients to a 1 h time period may result in overestimated downwind concentrations. It was found that the appropriate time interval for application of the horizontal PG dispersion coefficients varied widely depending on the corresponding meteorological variations. The approach of using a single-point estimate of σ_y, based on stability class and downwind distance and with no regard for observed variations in wind speed and direction, cannot account for the range of observed values of σ_y found in this research. Future research will detail how the methodology discussed in this article can be used to estimate horizontal dispersion coefficients that account for these meteorological variations.

REFERENCES

Barratt, R. 2001. *Atmospheric Dispersion Modeling: An Introduction to Practical Applications.* Sterling, Va.: Earthscan Publications.

Beychok, M. R. 1994. *Fundamentals of Stack Gas Dispersion*. 3rd ed. Newport Beach, Cal.: Milton R. Beychok.

Beychok, M. R. 1996. Air-dispersion modeling and the real world. *Environ. Solutions* 9(6): 24-29.

Brownell, F. W. 1999. Clean Air Act. In *Environmental Law Handbook*, ch. 5, 159-204. T. F. P. Sullivan, ed. Rockville, Md.: Government Institutes.

Cooper, C. D., and F. C. Alley. 1994. *Air Pollution Control: A Design Approach.* 2nd ed. Prospect Heights, Ill.: Waveland Press.

Gifford, F. A., Jr. 1961. Use of routine meteorological observations for estimating atmospheric dispersion. *Nuclear Safety* 2(4): 47-51.

Pasquill, F. 1961. The estimation of the dispersion of windborne material. *The Meteorological Magazine* 90(1063): 33-49.

Pasquill, F., and F. B. Smith. 1983. *Atmospheric Diffusion: Study of the Dispersion of Windborne Material from Industrial and Other Sources.* 3rd ed. Chichester, U.K.: Ellis Horwood.

Seinfeld, J. H., and S. N. Pandis. 1998. *Atmospheric Chemistry and Physics: From Air Pollution to Climate Change.* New York, N.Y.: John Wiley and Sons.

Trinity Consultants. 2000. Unpublished notes from dispersion modeling workshop: Practical Guide to Atmospheric Dispersion Modeling. Dallas, Texas: Trinity Consultants.

Turner, D. B. 1994. *Workbook of Atmospheric Dispersion Estimates: An Introduction to Dispersion Modeling.* 2nd ed. Boca Raton, Fla.: CRC Press.

U.S. EPA. 1996. Air quality criteria for particulate matter. EPA-600/P-95/001aF. Research Triangle Park, N.C.: U.S. EPA, Office of Health and Environmental Assessment, Environmental Criteria and Assessment Office. Available from: NTIS, Springfield, Va.: PB96-168232.

U.S. EPA. 2000. Meteorological monitoring guidance for regulatory modeling applications. EPA-454/R-99-005. Research Triangle Park, N.C.: U.S. EPA, Office of Air Quality Planning and Standards.

Venkatram, A. 1995. An examination of the Pasquill-Gifford-Turner dispersion scheme. *Atmospheric Environ.* 30(8): 1283-1290.

Williams, L. M. 1996. Evaluation of the Industrial Source Complex Screen2 for regulatory purposes. MS thesis. College Station, Texas: Texas A&M University, Department of Biological and Agricultural Engineering.

Zannetti, P. 1990. *Air Pollution Modeling: Theories, Computational Methods, and Available Software.* New York, N.Y.: Van Nostrand Reinhold.

Zwicke, G. W. 1998. The dispersion modeling of particulate for point and multiple point sources in agriculture. MS thesis. College Station, Texas: Texas A&M University, Department of Biological and Agricultural Engineering.